Astronomy & Astrophysics manuscript no. carretta
September 16, 2011 © ESO 2011

arXiv:1109.3199v1 [astro-ph.GA] 14 Sep 2011

A Strömgren view of the multiple populations in globular clusters

Eugenio Carretta[1], Angela Bragaglia[1], Raffaele Gratton[2], Valentina D'Orazi[2], and Sara Lucatello[2]

[1] INAF-Osservatorio Astronomico di Bologna, Via Ranzani 1, I-40127 Bologna, Italy
e-mail: `eugenio.carretta@oabo.inaf.it, angela.bragaglia@oabo.inaf.it`
[2] INAF-Osservatorio Astronomico di Padova, Vicolo dell'Osservatorio 5, I-35122 Padova, Italy
e-mail: `raffaele.gratton@oapd.inaf.it, valentina.dorazi@oapd.inaf.it, sara.lucatello@oapd.inaf.it`

ABSTRACT

We discuss a variety of photometric indices assembled from the *uvby* Strömgren system. Our aim is to examine the pros and cons of the various indices to find the most suitable one(s) to study the properties of multiple populations in globular clusters (GCs) discovered by spectroscopy. We explore in particular the capabilities of indices like m_1 and c_y at different metallicities. We define a new index $\delta_4 = (u - v) - (b - y)$ to separate first and second stellar generations in GCs of any metal abundance, since it keeps the sensitivity to multiple stellar populations over all the metallicity range and at the same time minimizes the sensitivity to photometric errors. We detecte clear differences in the red giant branches of the GCs examined, like skewness or bi/multi-modality in color distribution. We connect the photometric information with the spectroscopic results on O, Na abundances we obtained in our survey of GCs. Finally, we compute the effects of different chemical composition on the Strömgren filters and indices using synthetic spectra.

Key words. Stars: abundances – Stars: atmospheres – Stars: Population II – Galaxy: globular clusters – Galaxy: globular clusters: individual

1. Introduction

Thanks to the advent of efficient multi-object spectrographs at 8 m-class telescopes and consequent extensive surveys, in the last few years it has become clear that the presence of multiple stellar populations is ubiquitous in globular clusters (GCs) (see, e.g., Marino et al., 2008; Carretta et al., 2009a,b, 2010a,b, 2011; Johnson & Pilachowski, 2010). There are at least two generations of stars, the second one formed from the ejecta of a fraction of the first generation (the so-called polluters, see e.g., Gratton et al. 2001, 2004). This is a crucial piece of information on the early phases of evolution of GCs. It seems to be related to their intrinsic, specific formation mechanism (Carretta, 2006) and may give constrains to theoretical models of formation of massive stellar clusters.

With some delay with respect to spectroscopy, photometry is now also indicating the presence of different stellar populations (not necessarily of different age) in a subsample of clusters (see e.g. Anderson, 1998; Bedin et al., 2004). We will discuss some of its potentialities in the present paper, including strong sensitivity to abundances of some crucial element (namely N) and availability of large samples. However, most of the "hard" evidence concerning multiple populations in GCs is still based on spectroscopic surveys, where the multiple populations manifest through a distribution of stars along the Na-O, Mg-Al, and C-N anti-correlations, that have been found so far in *all* GCs where abundances of these elements in a large enough number of stars have been measured. Typically, modern spectroscopic surveys devoted to these studies include at best about 100 stars per cluster (e.g. Carretta et al., 2009a, and references therein) with internal errors in abundance, derived from intermediate and high resolution spectra, typically representing about 8-10% of the total variance. While various general information about early evolution of GCs can be obtained from such distributions (e.g. the number ratios between first and second generations and the total extent of the Na-O anticorrelation, see Carretta et al. 2009a, Carretta et al. 2010c), other require both larger samples and smaller internal errors. In particular, this is the case for the distinction between smooth continuous distributions and discrete ones. Such a distinction is crucial, because it provides a basic clue for the nature of the polluters, that might be either fast rotating massive stars (lifetime a few 10^6 yrs: Decressin et al., 2007) or the most massive among intermediate mass stars, undergoing hot bottom burning during their AGB phase (lifetime a few 10^7 yrs: Ventura et al., 2001). For instance, discrete distributions might be only compatible with the AGB polluters, as suggested by Renzini (2008).

Moreover, while multiple populations are an intrinsic property of *any* GC (so that this might be adopted as definition of a genuine GC, see Carretta et al., 2010c), the existing statistics shows also that *each* GC does show difference in the shape and extensions of the Na-O and Mg-Al anticorrelations. In other words, apart from a common nucleosynthetic pattern, each cluster is characterized by its particular history, whose features may be studied, in principle, with high resolution spectroscopy of a very large number of stars.

Alternative to spectroscopy, and less time consuming, photometry can provide both large samples and smaller internal errors. The most suitable photometric systems should couple a large sensitivity to the abundance variations related to the multiple population phenomena, with a good enough efficiency and the possibility to be applied to wide-field photometry. Sensitivity is obtained by passbands including strong molecular bands of CN (bandheads at 3883 and 4216 Å) or NH (around 3450 Å) or CH (around 4300 Å), since there are no common use filters sensible to the (smaller) spectral variations due e.g., to different Na abundances. Several photometric systems have been considered, including broad band (see e.g. Carretta et al. 2010d; Lardo et al. 2011), intermediate band (see Grundahl et al., 1999), and narrow band ones (Lee et al., 2009). these different methods have advan-

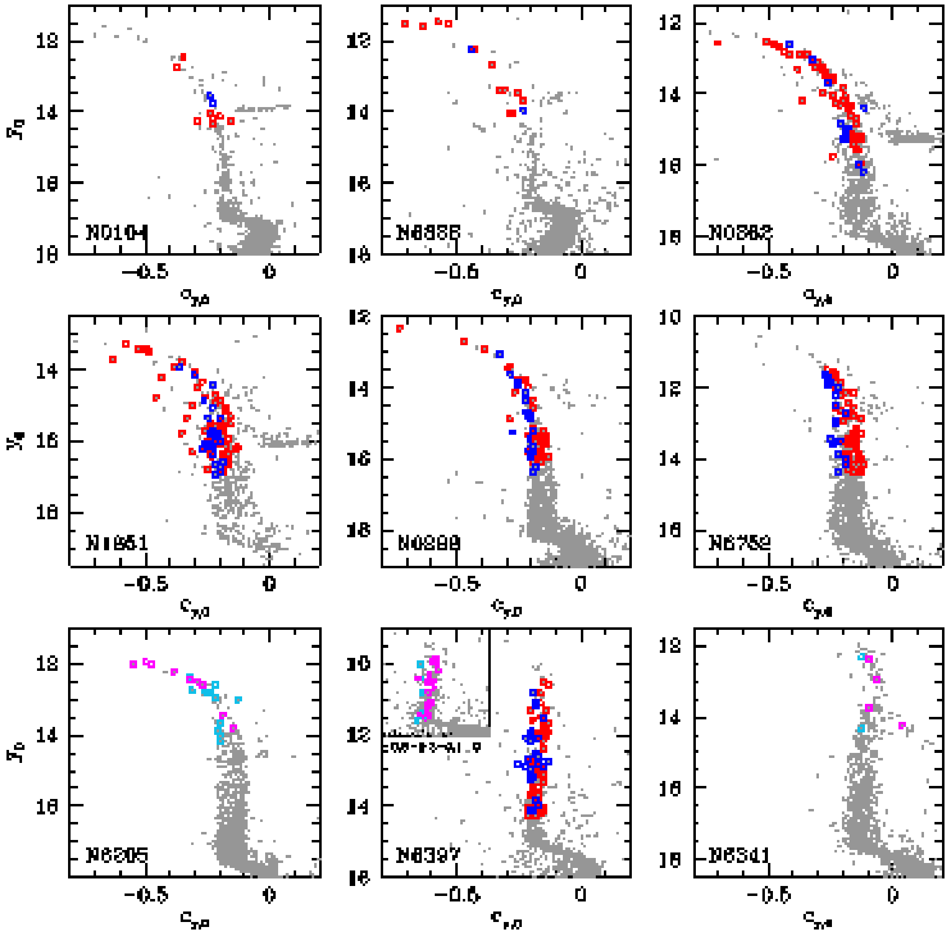

Fig. 1. CMDs in y_0,$c_{y,0}$ for the nine GCs, seven of which in common with our spectroscopic survey. Blue symbols indicate P stars and red symbols IE stars, all confirmed members on the basis of their RVs. For NGC 6205 (=M13) and NGC 6341 (=M92), whose spectroscopic data are not homogeneous to the seven other GCs, we use light blue and magenta, respectively; there are two suspect AGB stars in NGC 6205 and one confirmed HB star in NGC 6341 (note that the HB is redder than the RGB in these plots). For NGC 6397 we display in an inlet the results from Lind et al. (2009, 2011), shown on our same scale in magnitude, and on an expanded scale in $c_{y,0}$; the separation between Na-poor (light blue) and Na-rich (magenta) stars is perhaps cleaner, but is based on a smaller sample (about 30 stars).

tages and limitations: for instance Sloan filters (Stoughton et al., 2002) are very efficient, and high quality photometry can be obtained even for faint sources. However, sensitivity to the abundance variations is limited. On the other hand, while narrow band photometry may have very high sensitivity, results are not well understood yet (see Lee et al. 2009, and Carretta et al. 2010e). In this paper we will consider in more detail results from Strömgren photometry, extending the previous work by Grundahl et al. (1999) and Yong et al. (2008).

Strömgren photometry (Strömgren, 1956, 1966) has been originally devised for F-dwarfs and is applied mostly to the study of hot and intermediate spectral type (O to G) main sequence stars. There is however a long series of studies, (see e.g. Grundahl et al., 1998, 1999, 2002; Anthony-Twarog & Twarog, 2000; Anthony-Twarog et al., 2007) showing that it can be successfully used also for stars on the red giant branch (RGB) and on the horizontal branch (HB). In particular, Anthony-Twarog & Twarog (2000) briefly discussed the effects of the ”abundance anomalies” on the photometry of RGB stars in GCs. Grundahl et al. (1998) presented an extended Strömgren photometry of NGC6205 (=M13) and noted how the RGB stars presented a large spread in the c_1 index. They attributed it to the different chemical composition (not different iron content) of stars, since the relation between c_1 and CN, CH strength had already been demonstrated (e.g. in M 22 by Anthony-Twarog et al., 1995). A direct measure of N abundance was obtained by Yong et al. (2008) and was used to calibrate a new index c_y (see Sect. 2.1.1). A similar approach was followed for instance by Carretta et al. (2009a) that connected the c_y index to stars of the first (Na-poor) and of the second (Na-rich) generation in NGC 6752.

Sbordone et al. (2011) have recently presented a theoretical study of the influence of non-standard composition (e.g., enhanced in Na and/or He, and/or light elements like CNO) on the stellar models and the resulting isochrones, having in mind the particular case of the multipopulations in GCs. They considered the cases of Johnson *UBVI* and Strömgren *uvby* filters. We will discuss later (Sect. 5.1) the similarities and differences between their completely theoretical work and our observational approach. However, we note immediately that one of the most important is that they did all computations for a single metallicity[1]. value, near the average for the Galactic GC population,

---

[1] Within this paper, the term metallicity is usually adopted as a synonym of [Fe/H], with an overall abundance pattern characteristics of halo stars, that is with an excess of $\alpha-$elements.

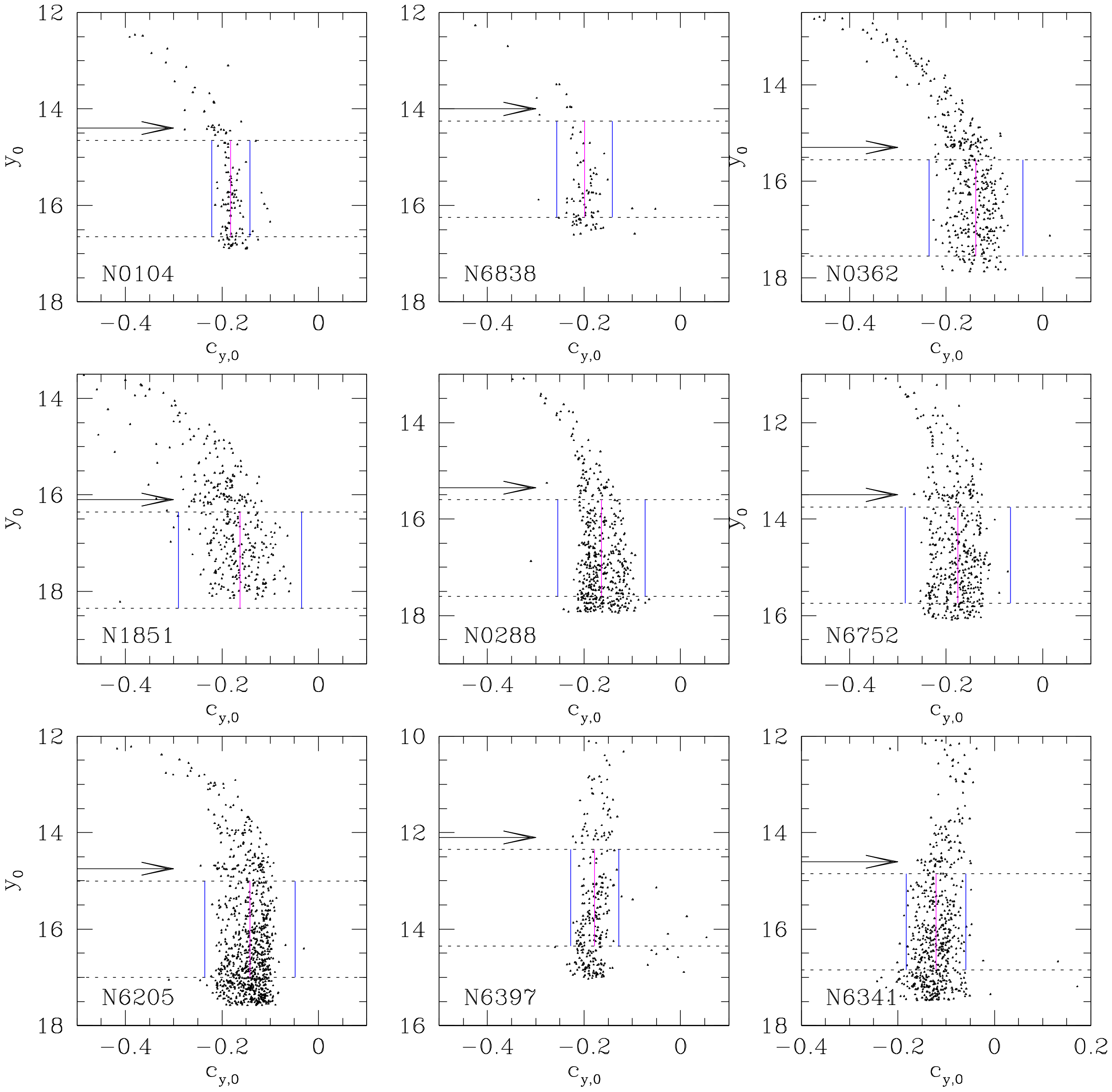

Fig. 2. Enlargement of the RGB region for the CMDs in y_0,$c_{y,0}$ of the nine GCs. An arrow shows the assumed magnitude of the RGB bump. The lines indicate the RGB stars selected to derive average and r.m.s. values for $c_{y,0}$ (see Sect. 4).

while we did instead consider GCs spanning (almost) the entire metallicity range for Milky Way GCs, from about −2.25 to about −0.70 dex.

In this paper we will systematically and deliberately try to determine whether photometric data, in particular in Strömgren filters, can be used to discriminate between stars of different stellar generations in GCs, by looking at their RGBs. We see that the situation is rather complex, and that there is a strong dependence on the evolutionary phase and the metallicity considered. For instance, the index c_y is efficient in separating different populations in GCs, but only at intermediate/low metallicity, while it loses sensitivity for metal-rich clusters (at least for the lower RGB). This sensitivity might even change its sign, making the interpretation of observational data ambiguous. The m_1 index is instead a good indicator of multiple populations at high metallicity. Finally, we explore the various indices that is possible to define and we select a new index δ_4 that uses all the four Strömgren filters *uvby*. We show that it is almost independent from reddening and that it can be used to efficiently separate different stellar generations in GCs over a large range in metal abundance.

The plan of the paper is as follows: in Sect. 2 we present the available data on which we base our analysis and we discuss the separation of GC stars in first and second generations as seen by the classical indices already known: c_y and m_1. In Sect. 3 we ex-

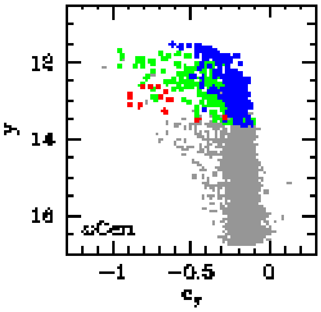

Fig. 3. CMD (not corrected for reddening) of ω Cen with stars of different [Fe/H] (from Johnson & Pilachowski 2010) indicated by different colors: blue stars have [Fe/H]< -1.6, red ones > -1, and green ones are in between.

Table 1. List of GCs.

GC	Other	[Fe/H]	E($B-V$)	y_0(RGB$_{bump}$)	Telescope
NGC 104	47 Tuc	-0.76	0.04	14.40	Danish
NGC 6838	M71	-0.82	0.25	14.00	NOT
NGC 362		-1.17	0.05	15.30	Danish
NGC 1851		-1.18	0.02	16.10	Danish
NGC 288		-1.32	0.03	15.35	Danish
NGC 6752		-1.55	0.04	13.50	Danish
NGC 6205	M13	-1.58	0.02	14.75	NOT
NGC 6397		-1.99	0.18	12.10	Danish
NGC 6341	M92	-2.25	0.02	14.60	NOT

Notes. [Fe/H]: Carretta et al. (2009c) and Carretta et al. in preparation for NGC 362; E($B-V$): Harris (1996); y_0(RGB$_{bump}$): this work.

amine other possibilities and present our new index δ_4, exploring its sensitivity to metallicity and to the properties of different stellar generations. In Sect. 4 we study the correlations between $c_{y,0}$ and δ_4 and cluster parameters. In Sect. 5 we interpret our results with the aid of synthetic spectra. A summary is given in Sect. 6.

2. The data

We used the publicly available Strömgren photometry for nine Galactic GCs collected by Grundahl and coworkers (Grundahl et al., 1998, 1999, 2002) and presented by Calamida et al. (2007), who used them to obtain a new calibration of the metallicity index m_1[2]. These data were obtained at two different telescopes (Nordic Optical Telescope –NOT– on Canary Islands, Spain, and Danish telescope on La Silla, Chile), as indicated in Table 1. Instruments covering very different fields of view (about 4′ and 11′ on a side) were used; sometimes a single field was targeted, sometimes two or more. The observations generally comprise the GC center, with the exception of the two most metal-rich cluster in the sample, NGC 104 (=47 Tuc) and NGC 6838 (=M71). We refer to the Calamida et al. (2007) paper for references and details on the observations and calibrations.

We made a selection on photometric errors and sharpness (a parameter used to separate well measured stars from galaxies, defects, and cosmic rays), retaining only those stars with errors in all the four filters ≤ 0.02 mag and $|\text{sharpness}| \leq 0.2$. We used the 2MASS Point Source Catalog (Skrutskie et al., 2006) to astrometrize the catalogues through software written by P. Montegriffo at the Bologna Observatory. We employed the E($B-V$) values from Harris (1996) and corrected the u, v, b, y magnitudes for reddening using the following relations $u_0 = u - 5.231 \times E(B-V)$, $v_0 = v - 4.552 \times E(B-V)$, $b_0 = b - 4.049 \times E(B-V)$, $y_0 = y - 3.277 \times E(B-V)$, with coefficients taken from Tab. 6 of Schlegel et al. (1998). From now on, all the quantities, colors, and combination of bands are intended as dereddened. For seven of the clusters the reddening is very low (E($B-V$)=0.02 to 0.05). It is slightly higher for NGC 6397, but only for NGC 6838 some differential reddening is present. Finally, we estimated the magnitude of the RGB bump visually inspecting the color-magnitude diagrams (CMDs); no sophisticated technique was applied, since this information is used only to roughly guide our selections (see below).

2.1. P, I, and E stars in Strömgren photometry

For seven of the clusters we obtained FLAMES spectra of RGB stars in our ongoing survey to study the Na-O anticorrelation in a large sample of GCs with different global parameters (see Carretta et al. 2007a for NGC 6752; Carretta et al. 2009a,b for NGC 104 (47 Tuc), NGC 6838 (M 71), NGC 288, and NGC 6397; Carretta et al. 2010b, 2011 for NGC 1851; Carretta et al., in prep. for NGC 362). We counter-identified stars in our spectroscopic samples, containing 50-150 objects each, and in the Strömgren catalogues. We generally found about 100 or more stars in common, except for NGC 104 and NGC 6838, where they are about 15. In the last two cases this is due to the fact that our FLAMES fiber configurations are positioned around the cluster center, whereas the photometric observations are located off the cluster center. We use these stars to try to understand whether it is possible to discriminate stars of first and second generation (primordial -P- and intermediate plus extreme -I plus E- respectively, in our notation: see Carretta et al. 2009a for the exact definition) on the basis of their position in color-magnitude diagrams (CMDs), experimenting several combination of filters. All stars analysed spectroscopically are members of the clusters, based on their derived radial velocities and chemical abundances.

For NGC 6205 (=M13) and NGC 6341 (=M92) we did a similar identification, using literature papers. For NGC 6205, a cluster presenting an extended Na-O anticorrelation (Sneden et al., 2004; Cohen & Meléndez, 2005), we used the measures of Na in Johnson et al. (2005) for the stars in common with our photometry (22 in total, two of which seem AGB, not RGB stars) to distinguish P and IE stars, since this paper includes more stars than the two cited above. For M92 there are no extensive studies of the Na-O anticorrelations (Armosky et al. 1994 measured Na and O in only nine stars), but 34 stars have Na abundances in Sneden et al. (2000). We counter identified objects in Sneden et al. with the photometric data and found six stars in common (one of them is an HB star).

2.1.1. The c_y index

Yong et al. (2008) defined the index c_y (see Table 2 for a summary of all the usual and new Strömgren indices used in the present paper) in their paper on NGC 6752; it traces the N abundance and was introduced because it is insensible to the temperature, at first order, as visible from the near-verticality of the RGB at least up to the level of the RGB bump (see Fig. 1). The dependence of c_y to N abundance comes from its definition, since it contains both the u filter, where the strongest NH bands are

---

[2] We downloaded the catalogues from the web page `http://www.oa-roma.inaf.it/spress/gclusters.html`

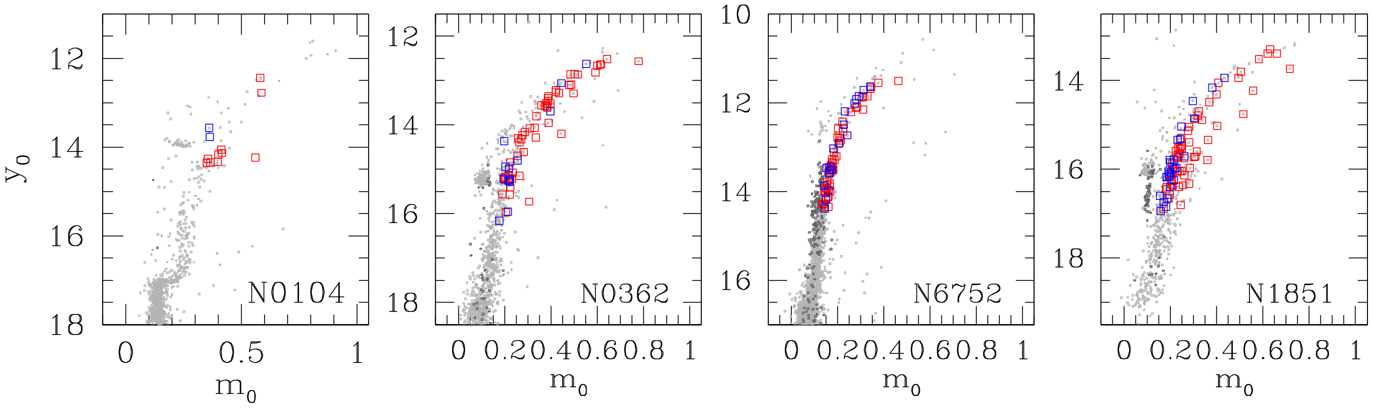

Fig. 4. CMDs in m_0, y_0 for three monometallic GCs and NGC 1851. Blue and red symbols have the same meaning of Fig. 1; darker grey points, visible for NGC 6752 and NGC 1851, are blue HB stars (as indicated by their $b - y$ color).

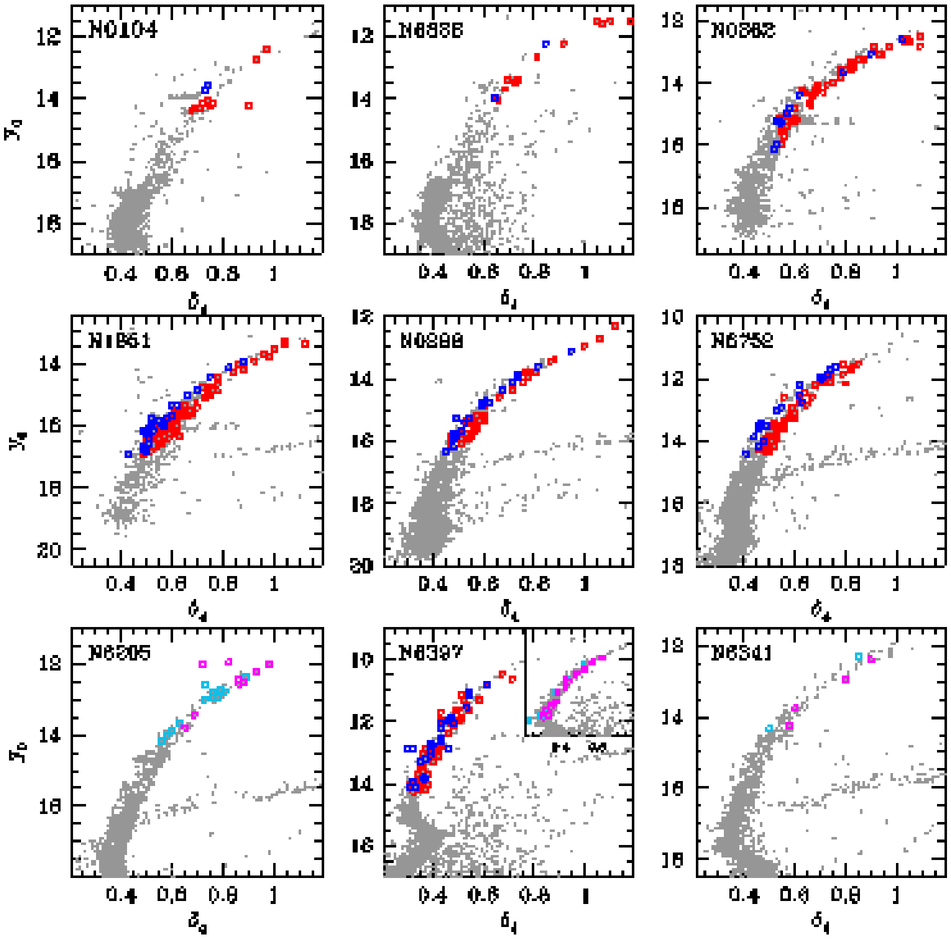

Fig. 5. CMDs in δ_4,y_0 (see text for the definition of δ_4). Blue symbols indicate P stars and red symbols IE stars (light blue and magenta for NGC 6205 (=M13) and NGC6341 (=M92)). Note that the HB is redder than the RGB in these plots for intermediate and low metallicity and that the blue HB and the blue stragglers are almost horizontal sequences. As in Fig. 1, for NGC 6397 we also show the results from Lind et al. (2009, 2011); the separation between Na-poor (light blue) and Na-rich (magenta) stars seems cleaner, due to the better data quality and the smaller sample.

present (at ∼ 3450 Å) and the *v* one, where the CN features are present (they are weaker but the filter is weighted twice in this index). Given the definition of c_y, we might then expect sensitivity to N abundance but also a complex behaviour. In fact, at low metal abundances and high temperatures only the NH contribution should be important, CN being negligible due to the combination of the quadratic dependence on metal abundances (N and C) and the strongest sensitivity to temperature of its formation. However, at high metallicity, absorption due to CN is much more relevant, and may dampen or even change the sign of the sensitivity of c_y on N abundances. More details are given in Sect. 5.

Table 2. Strömgren indices used in the paper.

Index	Definition	Alternative	Sensitive to:
m_1	$(v-b)-(b-y)$	$v-2\times b+y$	metallicity
c_1	$(u-v)-(v-b)$	$u-2\times v+b$	gravity
c_y	$c_1-(b-y)$	$u-2\times v+y$	gravity & N
δ_4	$(u-v)-(b-y)$	c_1+m_1	new index
δ_4’	$(\delta_4-\delta_{4B})/(\delta_{4R}-\delta_{4B})$		no $T_{\rm eff}$ dependence
δ_4”	$\delta_4'\times(\delta_{4R,b}-\delta_{4B,b})$		

Notes. δ_{4B} and δ_{4R} are the δ_4 values derived using the blue and red polynomial at the y_0 of each star (see text and Fig. 6). $\delta_{4B,b}$ and $\delta_{4R,b}$ are the same, but derived at the magnitude of the bump.

Fig. 1 shows the y_0,$c_{y,0}$ CMDs for the nine GCs, seven of which are in the FLAMES spectroscopic survey. As evident also from the enlargement of the RGBs presented in Fig. 2 (where the lines will be described in Sect. 4), the structure of the RGBs is different in the various clusters: the distribution in $c_{y,0}$ can be rather uniform and define a more or less tight sequence (as in NGC 104 (=47 Tuc) or NGC6341 (=M92)), or present a wide dispersion (NGC 1851), or show indications of skewness NGC 6205 (=M13) and bi-modality (NGC 288, NGC 6752). In Figure 1 we identify P and IE stars with different colors (blue for P and red for IE stars, and we maintain the color-coding throughout the paper). The P stars (i.e., Na and N-poor first generation stars) tend to lie on a tight sequence on the blue side of the RGB, while the I and E ones (i.e., Na and N-rich stars of the second generation), hereafter considered all together, occupy a larger color range on the red side. This is most evident in NGC 288, NGC 1851, and NGC 6752, and also clear in NGC 362 and NGC 6397. Note that in Carretta et al. (2009a) we could classify as P, I, and E only 16 objects for NGC 6397, because we conservatively required both Na and O abundances. However, to separate in P and IE populations, it is necessary to know only Na, so that we have all our 100 stars available for comparison. Only a few spectroscopically studied stars are present for NGC 104 and NGC 6838, but the two populations do not separate very clearly.

Such a segregation in color has already been found by Marino et al. (2008) in M4 (using the Johnson U filter); in NGC 6752 by Carretta et al. (2009a), where we identified the N-rich stars in Yong et al. (2008) with the Na-rich ones; and in NGC 6397 by Lind et al. (2011), using the Strömgren index c_y (and tightening the connection between abundance variations of different elements). The same effect (and the same explanation) was explored by Lardo et al. (2011) in nine GCs using the Sloan u filter.

Our first conclusion is therefore that $c_{y,0}$ *seems to efficiently separate sequences of first and second generation stars at intermediate to low metallicities (indicatively for [Fe/H]* $\lesssim -1.3$*), but does not work well for metal-rich clusters like NGC 104 or NGC 6838, or even NGC 362*. We will see in Sect. 5 that the effects of chemical abundances are complex.

In NGC 1851, even if the two stellar populations, P and IE, are segregated in $c_{y,0}$ along the RGB for $y_0 > 15.5$, the branch has a larger spread in Fig. 1 with respect to the other GCs. Recently Carretta et al. (2010b) presented the hypothesis that NGC 1851 is the result of a merger of two originally distinct GCs with slightly different metallicity, each one with a Na-O anticorrelation. The appearance of the plot would be explained if we are seeing the effect of a (small) spread in [Fe/H] and likely overall CNO content (Yong & Grundahl, 2008), with Na-O (hence N) differences in both the metal-rich and metal-poor components. That c_y measures both N and the overall metallicity is immediately visible using the template cluster with a dispersion in [Fe/H]: ω Cen. In Fig. 3 the most metal-poor population defines the right edge of the RGB, with stars of increasing metallicity populating sequences at more and more negative values of c_y (we used the stars studied by Johnson & Pilachowski 2010 with Strömgren photometry by Calamida et al. 2007). The spectral synthesis calculations reported in Sect. 5 show that a variation of [Fe/H] from -2.23 to -0.63, roughly the range observed in ω Cen, causes changes in c_y of 0.11 mag for subgiants and 0.18 mag for stars at the RGB bump, c_y being smaller in more metal-rich stars. Such differences in c_y are comparable to those expected between N-rich and N-poor stars. Similar differences are also produced by variations in the CNO content, within the limits that might be expected for stars in NGC 1851 and ω Cen (Yong & Grundahl, 2008; Marino et al., 2011). Disentangling these effects can be difficult without further information.

2.2. The m_1 index

The Strömgren index usually employed to trace the metallicity is m_1. In Fig. 4 we display the effects of metallicity using the m_1 index, or better its dereddened version, m_0, displaying three representative monometallic clusters and NGC 1851. In NGC 104 (=47 Tuc) the RGB has a spread in m_0, but this cluster is well known to have a negligible dispersion in [Fe/H] (e.g., Carretta et al., 2009c). Thus, this diagram indicates that the index m_0 is sensible also to the abundance of elements other than iron at high metallicity (e.g., N is present through the CN bands visible in the v filter, see discussion on c_y above and Sect. 5). This dependence is almost not detectable for NGC 362, similar in metallicity to NGC 1851, and is undetectable in the intermediate metallicity NGC 6752 (where the apparent spread of the RGB fainter than $y_0\sim13.5$ is due to the blue HB stars, which form an almost vertical sequence).

The P and IE stars occupy the bluer and redder parts of the RGB, respectively for NGC 104 (and NGC 6838=M71, not shown here), while the separation is much less clear in NGC 362 and is not seen at all for NGC 6752 (and the other clusters of similar or lower metallicity). In NGC 1851 there is also a spread, not imputable to the blue HB or simply to a metallicity difference, since the dispersion in [Fe/H] determined from spectroscopy should yield only a spread of 0.01 mag in the m_1 index, according to our spectral synthesis (see Sect.5). This cluster is very complex and many of its feature are discussed in (Carretta et al., 2011). Our second conclusion is then that m_0 *is a decent indicator of first and second generation, but only at high metallicity (indicatively for [Fe/H]* $\gtrsim -1.0$*)*.

To summarize the results of this discussion, the index c_y is a good indicator of different N abundances (i.e., distinct stellar generations) in metal-poor clusters. For metal-rich clusters, like NGC 104, the variations due to N in the $v-b$ and $u-v$ colors are similar and the net effect is to cancel or even to change the sign of the sensitivity of c_y to different populations; in this metallicity regime m_1 is a better indicator.

3. A new index, δ_4

To reduce as much as possible any degeneracy with metallicity, we test here a new Strömgren index, that we call δ_4, defined as $\delta_4 = (u-v)-(b-y)$, or $\delta_4 = c_1 + m_1$. We think that it can be an useful indicator for all metallicities, and that it minimizes the dependence on photometric errors, since it does not weight any of the photometric filters twice. Given the limit to photometric errors to < 0.02 mag adopted to select stars, the errors in δ_4

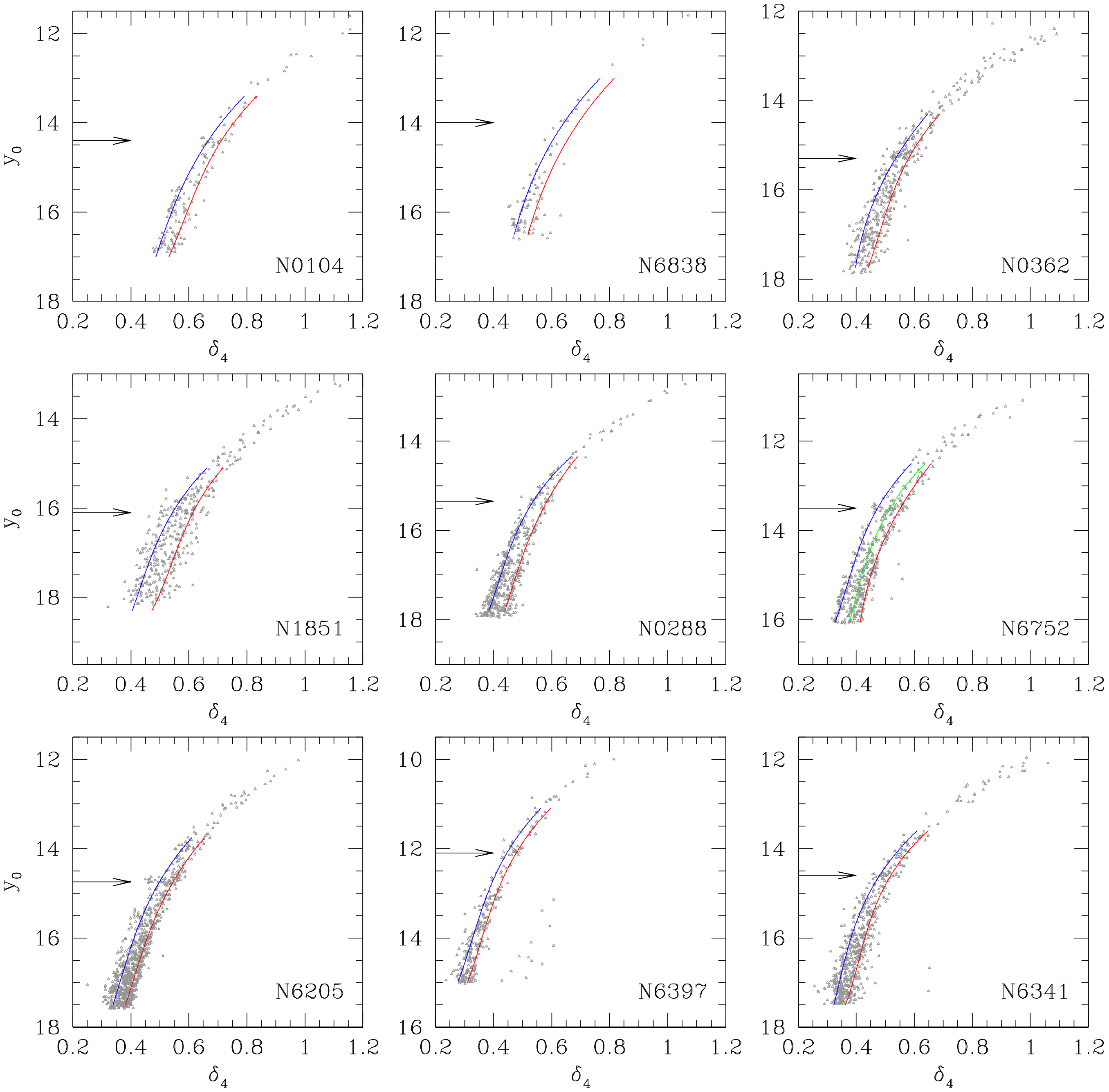

Fig. 6. CMDs in δ_4,y_0 for the RGBs of the nine GCs, with the RGB bump level indicated by an arrow. The blue and red curves, stopped one magnitude brighter than the RGB bump, where the statitics begins to be too scarce, are polynomials describing the populations, drawn according to the distributions of P and IE stars in Fig. 5. For NGC 6752 the distribution of stars is trimodal (see text and next figure) and an intermediate (green) line is drawn.

should be < 0.08 mag. However, a more realistic estimate is an r.m.s of ~ 0.02 mag. Furthermore, both m_1 and especially c_y do have a stronger weight on the bluest filters, the ones most probably having the largest photometric errors, especially for red stars. In our new index the photometric errors in $(u-v)$ and $(b-y)$ are not correlated with each other.

We have used in the present paper only dereddened values; however δ_4 would not depend much on reddening anyway. Taking from Strömgren (1966) the dependence on reddening for c_1 and m_1, we have that $E(\delta_4) = 0.02 \times E(b-y) = 0.014 \times E(B-V)$, i.e., δ_4 is approximatively reddening-free, at first-order approximation.

To test the ability of δ_4 to separate stars of different generations, we plot in Fig. 5 the δ_4,y_0 CMDs of the nine GCs, using the same symbols of Fig. 1; the figure shows that there is a good separation between P and IE stars. Also using this new index we

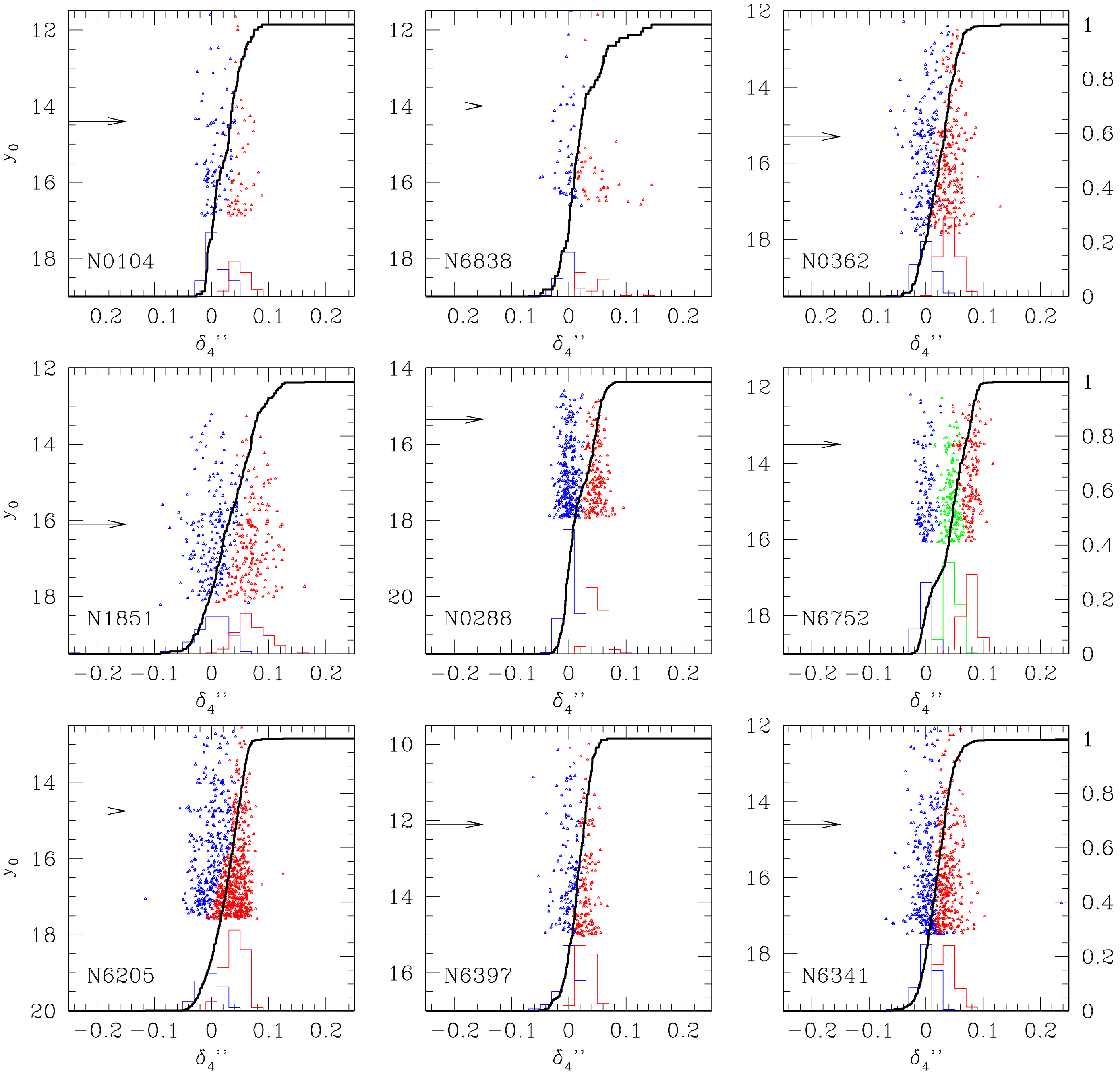

Fig. 7. Distribution in δ_4" for the nine clusters, showing the large difference among the GCs. The stars are colored in blue or red (and green, only for NGC 6752) according to the separation made in δ_4 (see previous figure); this division is only indicative. The colored histograms refer to the blue/red populations. The black, heavy lines represent the cumulative functions of all stars below the RGB bump, indicated by an arrow. These cumulative functions (to which the left y-axes refer) are the ones to consider to determine whether/where the distributions change slope because of a separation in color (i.e. population). The most notable cases are NGC 288, NGC 6752 (and maybe NGC 104 (=47 Tuc) and NGC 362).

see some structure in the RGBs, most evident for two clusters, NGC 288 and NGC 6752; there the distribution of stars in δ_4 seems bi-(multi)modal and not continuous. This is best shown by Fig. 6, where we display only the RGBs of all nine clusters on an enlarged scale. NGC 288 appears to have two distinct branches, one populated by P, the other by IE stars (see the previous figure), while NGC 6752 displays a tri-modal distribution (see also Fig. 7). If we trust the link between δ_4 and stellar generation, we could conclude that in NGC 288 there have been two episodes of star formation from gas well homogenized in each phase, without any appreciable continuous dilution from pristine gas, as invoked by models (e.g., Prantzos & Charbonnel, 2006) to explain the run of the observed Na-O anticorrelations. In NGC 6752 there are three populations, even if their separation is not so strikingly evident as in NGC 288.

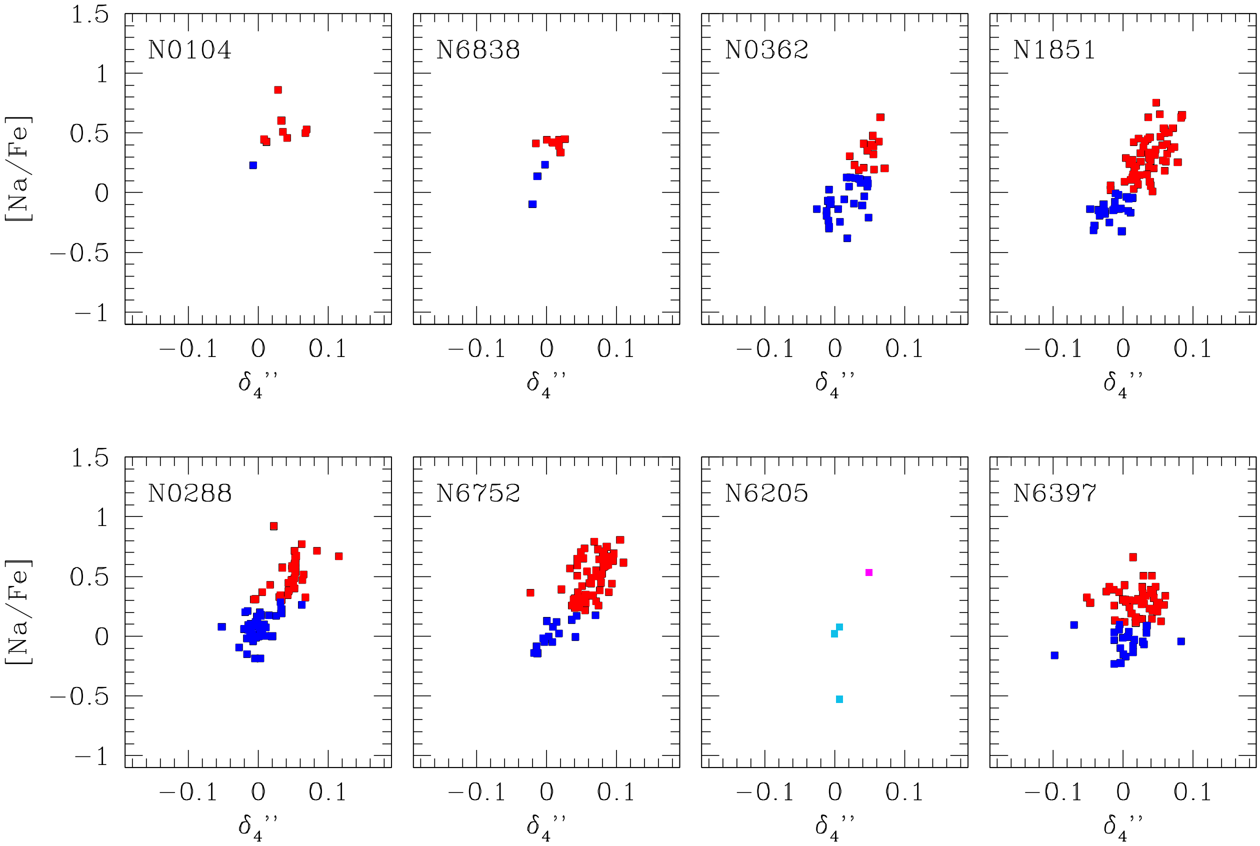

Fig. 8. Relation between δ_4" and the Na abundance for the seven GCs in our spectroscopic survey (and NGC 6205=M13, shown with different colors, like in Fig. 1). Blue and red symbols are for P and IE stars, respectively (the definition is based only on Na abundance, to increase the sample sizes).

The variation of δ_4 seems to depend on magnitude, i.e. on temperature (Figs. 5, 6) and also on metallicity, see next Section. Ignoring this effect would produce a blurring of the δ_4 values and there would be the risk of potentially hiding some real features. Guided also by the distribution of P and IE stars that we see in Fig. 5, we traced reference sequences in the δ_4,y_0 plane. First, we fitted a cubic polynomial in y_0 to the RGB ridge line; second, we labeled as "blue" the stars with negative residuals and "red" those with positive residuals with respect to it (P and IE stars, respectively); and finally we drew the best fitting cubic polynomial in y_0 to the two distributions of blue and red stars. The results are shown in Fig. 6 (where NGC 6752 is actually divided in three distributions).

These curves can help us to eliminate the curvature of the RGB using both the blue and the red sequences, and immediately compare the distributions of red and blue populations. We then define a new index, called δ_4' to rectify and normalize this index. Of course, with this procedure we risk to normalize to the errors in those cases where the intrinsic spread is small with respect to observational errors (like e.g. the case of NGC 6397). We then defined a second index δ_4'' which is δ_4' multiplied by the r.m.s. scatter around the best fit line for the whole sample (see Table 2 for definitions). δ_4'' takes into account the fact that the blue and red sequences can be more or less separated in color in different clusters. This index can be used to better identify the presence of multiple distributions along the RGBs. Note that given its definition, photometric errors on δ_4'' should be similar to those in δ_4, with typical r.m.s values of ~ 0.02 mag.

We also note that δ_4' and δ_4'' are only defined within a limited range in magnitude for each cluster, and extrapolation of the best fit lines out of these regimes produce results that are clearly wrong. Our following discussion only considers those stars fainter than the RGB bump (or slightly brigther).

3.1. δ_4 and the separation of star generations

Fig. 7 shows the RGBs of the nine GCs "rectified" by using this new index, and allows to appreciate that strong differences do exist among the GCs in our sample. This division is rather artificial in most cases: we simply divided second generation (redder) and first generation (bluer) stars by choosing the stars that lie near the red and blue lines in Fig. 6. The clear exceptions are NGC 288 and NGC 6752, since the distribution of giant stars is clearly bimodal in the first one, and tri-modal in the latter. NGC 104 (=47 Tuc) and NGC 362 show smaller indication of separation, although a bi-modal distribution is not excluded; NGC 6205 (=M13) has perhaps the larger fraction of IE stars; and NGC 1851 has the largest dispersion in δ_4'', possibly in agreement with the hypothesis of an origin by merger of two clusters with different chemical composition (Carretta et al. 2010b, 2011).

To effectively see whether we can really discern a separation of populations, in the same figure we also present the cumulative distribution in δ_4" (limited to stars below the RGB bump). A change in the slope is an indication of separations into discrete distributions; NGC 104, NGC 288, and NGC 6752 are the only three GCs where such a feature is clearly present (and maybe NGC 362).

Only in the most evident cases of NGC 288 and NGC 6752 we estimated the fractions of second (red, red plus green in the latter) and first generation (blue) stars as defined by the photometry and the δ_4 (and δ_4”) index and compared them with the corresponding fractions of P and IE stars, defined spectroscopically. In Carretta et al. (2009a) we found that for all GCs the fraction of P stars is more or less constant, at a level of about one-third. Here we find the same result for NGC 6752 (blue stars=27%, red stars=73%, compared to P=27% and IE=73%). However, for NGC 288 the fractions of P and IE stars are reversed (62% and 38% from the photometry compared to 33% and 67% from the spectroscopy). The split in the RGB of NGC 288 is very clear (and is present, in the same sense, also in the $c_{y,0}$,y_0 CMD). There are several considerations to be taken into account. First, the discrepancy is reduced if we classify stars in P and IE using only Na abundances, since in this case we have fractions of 42% and 58%, respectively, Second, in NGC 288 the spectroscopic sample is limited, perhaps more than in other GCs, to stars significantly brighter than the bulk of the photometric sample, while the stronger concentration of blue/P stars is at the fainter limit of the RGB, where the actual separation is less evident. Third, we see in Figs. 1 and 5 that, at the fainter limits of the spectroscopic sample, there are a few IE stars that overlap in color the P ones (the reverse does not happen). In this particular cluster the division in color/index is quite natural, while the spectroscopic classification in P and IE rests on the less defined minimum value for Na (see Carretta et al., 2009a, for a definition); indeed, a slightly different separation in Na would bring the fractions of P and IE stars more in agreement with the photometric ones. In conclusion, the result we found on the relative importance of first and second generation stars (one third and two thirds) is statistically valid on the whole sample of GCs, but in some clusters there may be individual variations. While this issue merits attention and further considerations, this is besides the scope of the present paper.

Since the separation between populations mostly rests, spectroscopically, on the Na abundance, we plot in Fig. 8 the relation between δ_4” and the Na abundance, which is rather tight. Here we have divided stars in P and IE using only Na abundance, to increase the samples (we checked that this approach does not generally make a significant difference with respect to the criteria for PIE classification as adopted in Carretta et al. 2009a) and we also restrict to stars below the RGB bump since the separation between the sequences, hence the definition of δ_4”, is better. We also show the case for NGC 6205 where, however, most of the observed stars are very bright. Nothing can be said for NGC 104, and NGC 6838 (=M71) since we have too few stars. For the other GCs, there is a very good correlation between the δ_4” index and Na, especially for the intermediate metallicity ones (the sensitivity is worse at very low metallicity, like for NGC 6397, where abundances are derived from rather weak lines). The relations could be interpreted as continuous, but we see the possibility of separating stars in two groups, again most clearly in NGC 288 and NGC 6752, but also in NGC 1851 and especially in NGC 362 (where neither δ_4” or Na show well defined partitions). It is sounder, and more natural, to separate the populations using *both* photometric and spectroscopic information, whenever possible.

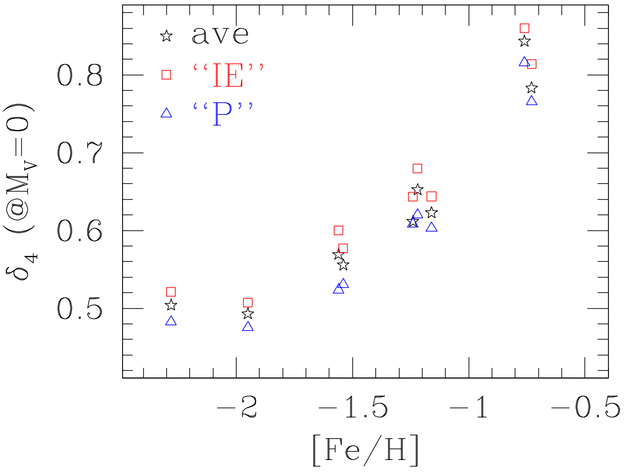

Fig. 9. Relation between metallicity and the value of δ_4 at the reference magnitude $M_V = 0$ (i.e., at about the HB level) computed for the whole RGB and for the blue and red stars (P and IE, respectively).

3.2. δ_4 and metallicity

Both m_1 and c_y have a (complex) dependence on metallicity ([Fe/H] and N abundance). To explore what is the dependence of δ_4, we have measured the value of δ_4 at a reference magnitude ($M_V \simeq M_y = 0$, i.e., near the level of the HB) and for the different populations, computing three δ_4 values (blue, average, and red), guided by the natural separations and the lines drawn in Fig. 6. Given the rather good correlation existing between δ_4” index and Na abundances, we label the blue and red lines as P and IE respectively, even though it should be clear that the definition of PIE groups should be based on spectroscopy rather than on photometric data.

The values we obtain by this procedure for the clusters we examined are plotted in Fig. 9. We see that δ_4 has a strong dependence on metallicity. The whole range of δ_4 observed in NGC 6752 can be obtained if the metallicity varies by about 0.3 dex (i.e., the difference between NGC 6752 and NGC 288). We then expect some difficulties in separating N-rich and N-poor populations in clusters like NGC 1851, where there is an internal spread in metallicity (Yong & Grundahl 2008 and Carretta et al. 2010b find a scatter of about 0.08 and 0.07 dex, respectively, well above the expected uncertainties). We conclude that δ_4 is a very good estimator of the N abundance if a cluster is monometallic, as almost all are, at least at the precision we can reach with the present day spectra and analysis methods (in Carretta et al. 2009c we showed, using UVES spectra of 19 GCs, that the internal homogeneity is at about 10%, given an upper limit to the scatter of iron of less than 0.05 dex). Where this is not valid, as in NGC 1851, it is better to separate the dependence from [Fe/H] and N using, e.g., m_1. Of course, δ_4 also has a dependence on temperature, as seen from the curvature of the RGBs.

4. $c_{y,0}$, δ_4 and cluster parameters

We have explored the possible relations of the $c_{y,0}$ and δ_4 indices with global cluster parameters. For $c_{y,0}$, we concentrated on the stars below the RGB bump where the distribution in $c_{y,0}$ is almost vertical, i.e. independent of the temperature (Fig. 2).

As already discussed, the distribution in $c_{y,0}$ is different from cluster to cluster and may present evidence of structures. These findings, given the connection between this index and N, must be indicative of different distribution in N-richness among the GCs.

For each GC we chose only stars in a two-magnitude bin below the RGB bump (i.e., $y_{bump}+0.25$ to $y_{bump}+2.25$) and selected as RGB those falling within 3σ from the average $c_{y,0}$ value (after a κ-*sigma* clipping); the selected region is indicated in the figure. The adopted criteria allow us to deal with statistically significant samples of stars and the verticality of the RGB in this plane allows us to separate rather easily the possible contamination by field stars. We measured the average value of $c_{y,0}$ in the defined interval and its r.m.s. scatter. In principle, we expect that a higher average value does indicate a higher relative weight of the second generation, while a larger r.m.s. scatter could be the signature of a larger contribution of the nuclear processing by the first generation polluters to the yields budget in the cluster.

We show the best correlations we found for the average $c_{y,0}$ and its r.m.s. in Fig. 10. As expected and also already visible from Fig. 2, the average depends on metallicity (left panel in second row of Fig. 10). We have tried to see if there are other significant correlations with several structural or chemical properties, but results are not very robust. The average increases somewhat with the cluster mass (represented by its proxy, the total absolute visual magnitude M_V), and it is larger where the Na-O anticorrelation is more extended (as indicated by the interquartile ratio IQR([Na/O], see Carretta et al. 2009a). Similarly, it is related to δY, the amount of He-enhancement that can explain the long blue HB tails (Gratton et al., 2010) and which is connected with the extension of the Na-O anticorrelation. Some correlation exist with the relaxation time at half-mass radius, once 47 Tuc (which has the longest relaxation time in the sample) is excluded (rightmost, upper panel of Fig. 10). A full cluster relaxation occurs in at least 2-3 relaxation times and considered the age of 47 Tuc (see, e.g., Gratton et al., 2010) this GC should be fully relaxed.

We note that 47 Tuc was already indicated by Carretta et al. (2010c) and Gratton et al. (2010) to be a peculiar cluster, with rather small values of IQR[Na/O] and He spread with respect to other clusters of similar total mass. The same is apparently visible in the correlation of the average $c_{y,0}$ index and M_V in the present data. Recently, Lane et al. (2010) suggested that also this cluster might be the result of a past merger of two originally distinct clusters. However, we must point out that for 47 Tuc the number of stars is smaller than in the other GCs, given the more external region sampled by the available Strömgren photometry. It is possible that at such larger distances from the cluster center, the ratio first-to-second generation stars is shifted toward the primordial population, as expected on theoretical grounds (e.g., D'Ercole et al., 2008) and as seen e.g., from the distribution of CN-rich stars (Norris & Freeman, 1979), interpreted as Na-rich, second-generation ones in the present-day framework.

The last row of panels in Fig. 10 shows the best correlations we found using the dispersion in the $c_{y,0}$ index. In the case of the r.m.s. scatter, the correlations with the spread of He δY (from Gratton et al. 2010) and IQR([Na/O]) are significant at more than 99%; the first is mirrored by the anticorrelation between the spread in $c_{y,0}$and the M$_{min}$, the minimum mass reached along the HB (also from Gratton et al. 2010).

These findings represent another indication that c_y is tied to the different generations through its sensibility to N (and the link with Na, O, and He abundances).

A similar approach can be taken for δ_4, and we show in Fig. 11 the results. Also in this case we used stars below the RGB bump and determined the average and r.m.s. (we used here the median, given the less uniform distribution in this index) of δ_4" for the nine clusters. The indications are similar to the previous case for M_V, IQR, δY, and M$_{min}$, while the correlation with the relaxation time disappears.

5. Comparison of observed colors with synthetic spectra: interpretation

In order to better understand the observed runs of the classical and new indices we obtained from the Strömgren system, we computed a number of synthetic spectra over the wavelength region of interest (approximately, $\lambda = 3000 - 6000$ Å) for some cases of interest. The synthetic spectra were computed using the Kurucz (1993) set of model atmospheres (with the overshooting option switched off), and line lists from Kurucz (1993) CD-ROM's. It is well known that this line lists, while very extensive and useful, still have important limitations. In addition, both the model atmospheres and our syntheses include approximations (e.g. mono-dimensional atmospheres, scattering treated as an additional absorption, etc.). For this reason we only consider differential effects between stars that should be very similar, except for details of the chemical composition.

All synthetic spectra were computed with a wavelength step of 0.02 Å. Then they were convolved with a Gaussian with a FWHM of 2 Å, and rebinned at about 1 Å sampling for an easier handling and display. The spectra were finally convolved with the transmission of the *uvby* (Strömgren, 1956) and *Ca* filters (Anthony-Twarog et al., 1991), collected in the Asiago Database on Photometric Systems (Moro & Munari, 2000).

For all choices of atmospheric parameters, we considered as reference the spectra computed with the typical abundance pattern observed in field metal-poor stars, that is [C/Fe]=[N/Fe]=0, [O/Fe]=[Mg/Fe]=[Ca/Fe]=0.4, and [Ti/Fe]=0.2. Spectra computed with these parameters are labeled "N-poor". They should mimic the composition of P stars according to Carretta et al. (2009a). For the same choices of atmospheric parameters, we computed spectra for atmospheres having [C/Fe]=−0.2, [N/Fe]=+1.3, and [O/Fe]=−0.1 (and the same abundances for Mg, Ca, and Ti). We labeled this second group of spectra "N-rich"; they should mimic the spectra of I stars.[3] In addition, we also explored in a more limited way the influence of C increase, computing spectra for [C/Fe]=0.2, [N/Fe]=0.0, [O/Fe]=0.4 ("C-rich,N-poor" spectrum) and [C/Fe]=0.2, [N/Fe]=1.3, [O/Fe]=-0.1 ("C-rich,N-rich" spectrum). All these compositions are also indicated in Table 3.

First we considered pairs of "N-poor" and "N-rich" spectra for the four metallicities [Fe/H]=−2.23, −1.63, −1.23, and −0.63. They have effective temperature $T_{\rm eff}$ and surface gravity $\log g$ appropriate for stars at the base of the subgiant branch (SGB), at the RGB bump, and at $M_V = -1$ (as read from the isochrones of log(age)=10.10 by Bertelli et al. 2008). Table 3

---

[3] We do not expect any significant change between I and E stars in this respect, insofar the abundance of O is larger than that of C. The main difference between I and E stars is in the O abundance, which changes from [O/Fe] about −0.1 to about −1, but even in this case spectroscopic observations do not indicate the presence of very strong C-bands, which are expected as soon as the abundance of C exceeds that of O. The filters we are considering do not contain OH bands (e.g., the strong ones near 2700 Å) but only N molecules. However, N is already about 90% of the whole sum of CNO elements in I stars, and the small further increase expected between I and E stars (about 5%) does not influence our computations.

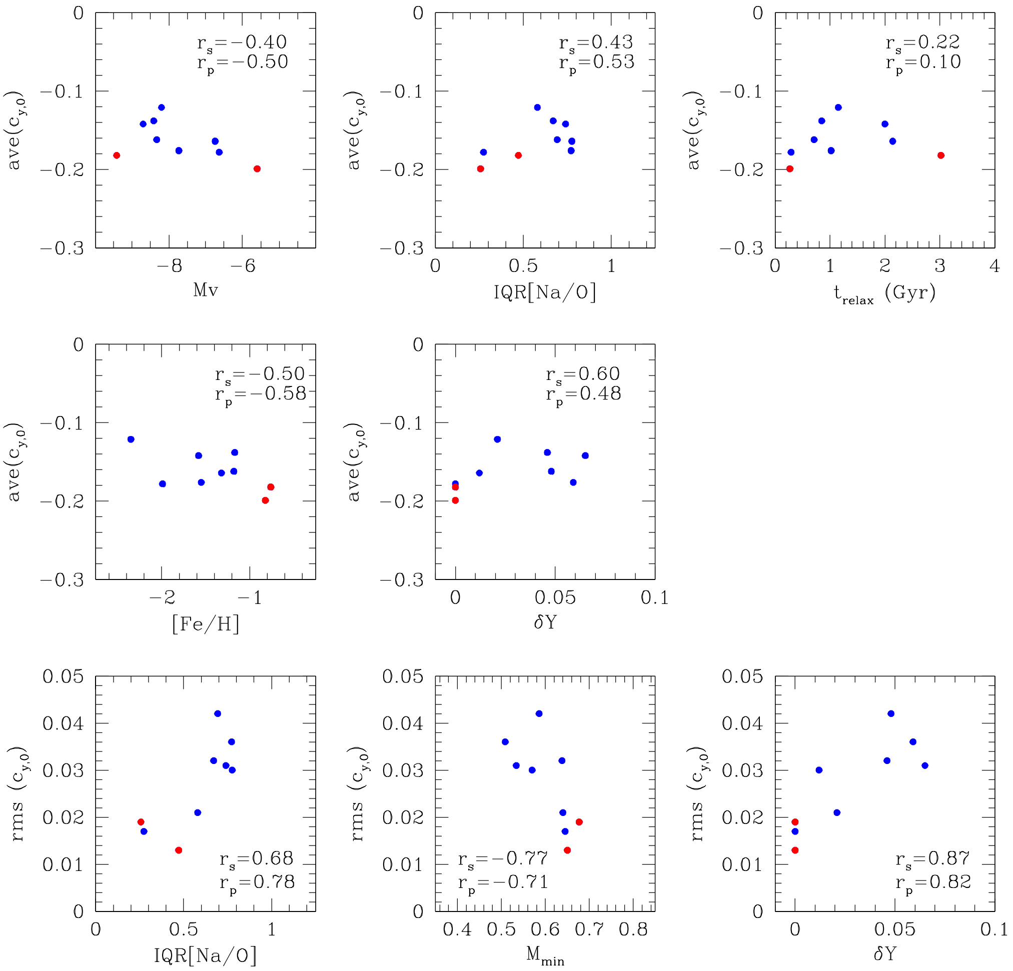

Fig. 10. Correlations of the average and r.m.s. for $c_{y,0}$ with some interesting parameters; the two metal-rich clusters are indicated by red points. r_S and r_P are the Spearman's rank and Pearson's linear correlation coefficients, respectively. The only highly significant correlations (significance of the Pearson coefficient larger than 99%) are with metallicity for the average value of $c_{y,0}$ and with IQR([Na/O]), $M_{\rm min}$ and δY for its r.m.s..

lists the values of the atmospheric parameters we used and the offset in magnitude between the "N-poor" and "N-rich" spectra for the *uvby* and *Ca* bands and for various photometric indices (m_1, c_1, c_y, and δ_4).

Figure 12 presents an example for the synthetic spectra appropriate to stars at the RGB bump (panel a) and above the RGB bump (panel b) for [Fe/H]=−1.23; the transmission of the filters is also shown. This figure visually demonstrates what has already been discussed in the previous sections. The differences between the "N-poor" and "N-rich" spectra are essentially due to the different strength of the molecular bands: the NH band at ~ 3400 Å, which is stronger in the "N-rich" spectra and falls within the *u* band; and the CN violet band at ~ 4216 Å, which falls within the *v* band. The CH A-X band at ~ 4320 Å is also different between the two spectra, but is near the edge of the *v* band, so that its impact on the Strömgren colors is very small. As a consequence, the flux predicted for both the *v* and the *u* bands is smaller for the "N-rich" spectra than for the reference "N-poor" ones. The difference is larger for the *u* band, where it may be as much as 0.2 mag, save for the coolest and more metal-rich stars, where the effect is larger in the *v* band. This is due to both saturation and different temperature sensitivity of the molecular bands. A sketch of the variations in the u, v, b, y, Ca filters and in the three indices m_1, c_y, and δ_4 is presented in Fig. 13 where we can appreciate their different sensitivity to CNO abundances along the various evolutionary phases and their run with metallicity. Table 3 and Fig. 13 can be used to interpret what we have seen in the observed CMDs in term of different chemical composition (in other words, of different stellar population).

While the largest variations between first and second generation stars are expected for N, also the C variations can have an effect on the photometry. We computed only a couple of spectra, and Fig. 12 shows also the results a for C-enhanced composition. The corresponding differences in the various filters/indices are indicated in Table 3. From these computations we see that, for N-poor stars the effect of an increased C abundance is small, since the CN bands are not very strong and O is much more abundant than C in any case. On the contrary, for N-rich stars, an enhancement in C produces large changes to the Strömgren magnitudes, especially for the *u* and *v* filters. This means large differences in indices like c_y and m_1 (while the differences al-

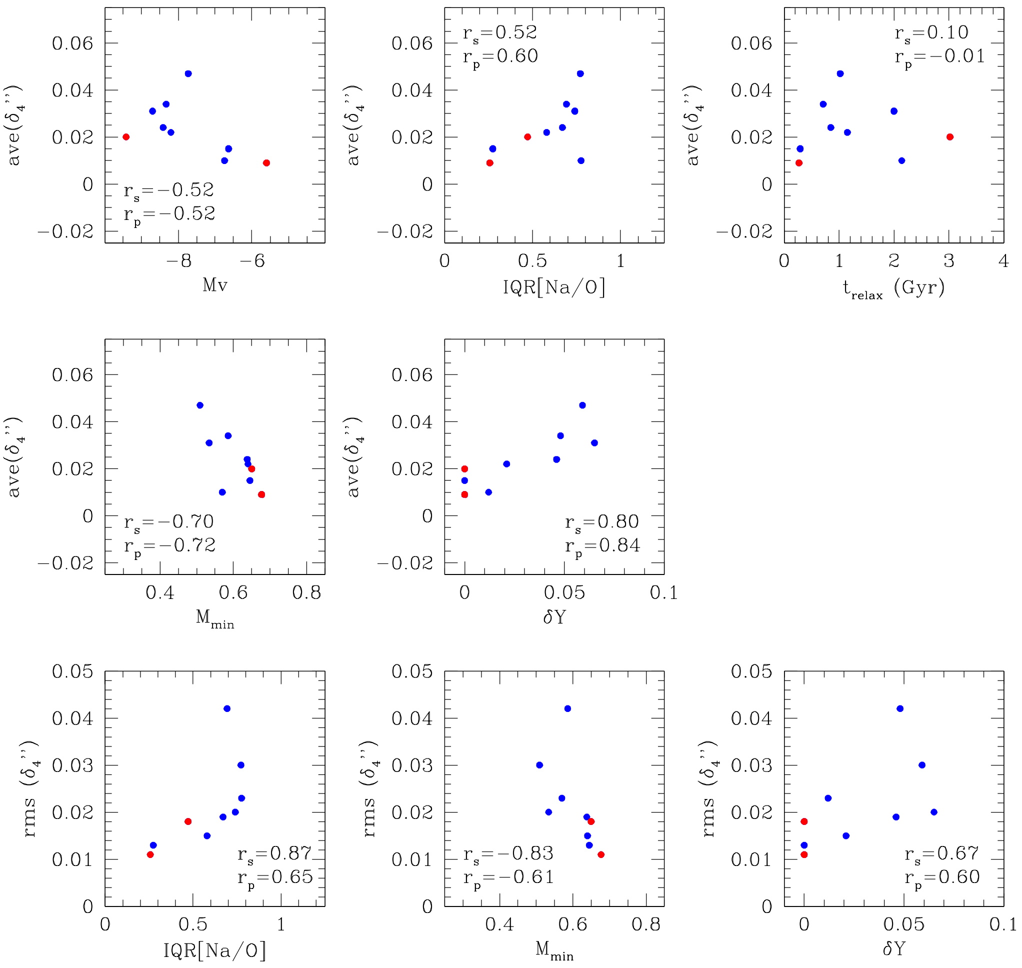

Fig. 11. Correlations of the median value and r.m.s. for δ_4 with some interesting parameters. Symbols are as in previous figure.

most cancel out for δ_4, since it is the sum of the previous indices, whose variations have opposite sign).

The combination of N and C variations could then explain some peculiar cases, like NGC 1851, where we see cluster stars lying along an "anomalous", less populated RGB (see e.g. Fig. 4). In this cluster there have been (controversial) claims of variations of the sum of C+N+O; this will be discussed in a paper in preparation. Here we simply propose that these stars could be the ones which are both C and N-rich, while the ones which have lower N abundance fall in with the bulk of the stars, even if C-rich.

Finally, we considered another possible composition difference; at the RGB bump there is a change in the surface abundance of C and N (see e.g., Gratton et al., 2000), i.e., C decreases and N increases, due to a mixing episode. In C-normal, N-poor stars the increase in N after the RGB bump almost compensates the decrease in C, and the CN bands do not change their strength. Instead, in C-normal, N-rich stars, the N abundance is already high and the N increase has proportionally a smaller impact and does not compensate enough the decrease in C. Hence, there is a smaller difference between a N-rich and N-poor star if we take into account the evolutionary changes (see the correspondingly smaller differences in *u* and *v* and all correlated indices).

Armed with these results, we may then examine the prediction of our spectral synthesis on the observed indices.

$m_1 = (v-b)-(b-y)$ is the classical metallicity index of the Strömgren photometry. In the present context, we notice that *b* and *y* (hence $b-y$, the classical temperature indicator) are insensitive to variations in the abundances of the CNO elements. For m_1, the only dependence is then contained in the *v* magnitudes. Since the CN violet band is very weak in metal-poor and/or warm stars, m_1 separates "N-poor" and "N-rich" only for cool, metal-rich stars.

$c_1 = (u-v)-(v-b)$ is the classical gravity index of Strömgren photometry, measuring the Balmer jump. In the present context, it essentially measures the difference between the strength of the NH and CN violet bands (the latter actually weighted twice). Therefore it separates well "N-poor" and "N-rich" at low metallicities (where the CN violet band is negligible), but it changes the sign of its sensitivity for cool metal-rich stars, where the CN violet band is quite strong. The same holds for c_y ($= c_1-(b-y)$), which has the same sensitivity on CNO abundances of c_1.

Our new index $\delta_4 = (u-v)-(b-y)$ keeps constant the sign of its sensitivity to CNO abundances over a range of temperature/metallicity/gravity larger than for m_1 and c_1 or c_y, although it also fails for the coolest and most metal-rich stars. The reason of this more uniform behavior is that it weighs only once the *v*

Table 3. Model sensitivity of Strömgren photometric indices.

Phase	$T_{\rm eff}$	$\log g$	[A/H]	Δu	Δv	Δb	Δy	$\Delta CaII$	Δm_1	Δc_1	Δc_y	$\Delta\delta_4$	C-normal,N-poor minus
SGB	5578	3.44	-2.23	-0.056	0.002	0.000	0.000	0.003	0.002	-0.061	-0.061	-0.059	C-normal,N-rich
RGB-bump	5018	2.00	-2.23	-0.082	0.003	0.001	0.000	0.003	0.001	-0.088	-0.089	-0.086	C-normal,N-rich
$M_V = -1$	4857	1.60	-2.23	-0.087	0.001	0.000	0.000	0.003	0.001	-0.090	-0.090	-0.089	C-normal,N-rich
....	....	....	....	-0.062	-0.003	0.000	0.000	0.003	-0.003	-0.056	-0.056	-0.059	(a)
SGB	5537	3.53	-1.63	-0.099	-0.007	0.000	0.000	-0.002	-0.007	-0.086	-0.086	-0.092	C-normal,N-rich
RGB-bump	5001	2.19	-1.63	-0.144	-0.043	0.000	0.000	-0.005	-0.043	-0.059	-0.059	-0.102	C-normal,N-rich
$M_V = -1$	4683	1.51	-1.63	-0.175	-0.102	-0.002	0.000	-0.007	-0.101	0.027	0.028	-0.071	C-normal,N-rich
....	....	....	....	-0.096	-0.043	0.000	0.000	-0.005	-0.043	-0.009	-0.009	-0.052	(a)
SGB	5369	3.44	-1.23	-0.138	-0.022	0.001	0.001	0.000	-0.023	-0.093	-0.093	-0.116	C-normal,N-rich
RGB-bump	4948	2.42	-1.23	-0.176	-0.076	0.001	0.000	-0.002	-0.078	-0.023	-0.024	-0.101	C-normal,N-rich
....	....	....	....	-0.221	-0.163	-0.010	-0.002	-0.012	-0.161	0.096	0.103	-0.050	C-rich,N-rich
$M_V = -1$	4478	1.40	-1.23	-0.189	-0.149	-0.002	0.000	-0.006	-0.145	0.107	0.109	-0.038	C-normal,N-rich
....	....	....	....	-0.014	-0.025	-0.006	-0.002	-0.021	-0.015	0.030	0.034	0.015	C-rich,N-poor
....	....	....	....	-0.251	-0.274	-0.027	-0.006	-0.021	-0.226	0.270	0.291	0.044	C-rich,N-rich
....	....	....	....	-0.162	-0.103	-0.001	0.000	-0.006	-0.101	0.042	0.043	-0.058	(a)
SGB	5229	3.71	-0.63	-0.190	-0.110	-0.001	0.000	-0.003	-0.109	0.029	0.030	-0.080	C-normal,N-rich
RGB-bump	4765	2.53	-0.63	-0.211	-0.180	-0.003	0.000	-0.007	-0.175	0.146	0.149	-0.029	C-normal,N-rich
$M_V = -1$	4016	1.08	-0.63	-0.153	-0.176	-0.005	-0.001	-0.011	-0.166	0.193	0.197	0.027	C-normal,N-rich
....	....	....	....	-0.097	-0.123	-0.002	0.000	-0.011	-0.118	0.146	0.148	0.028	(a)

Notes. (a) Δ computed as C-normal,N-poor minus C-normal,N-rich, but with a composition changed after the RGB bump for C,N.
C-normal,N-poor stars have: [C/Fe]=[N/Fe]=0, [O/Fe]=[Mg/Fe]=[Ca/Fe]=+0.4, [Ti/Fe]=0.2;
C-normal,N-rich stars have [C/Fe]=−0.2, [N/Fe]=+1.3, [O/Fe]=−0.1 (and the same abundances for Mg, Ca, and Ti);
C-rich,N-poor stars have [C/Fe]=+0.2, [N/Fe]=0.0, O and other elements as in first case;
C-rich,N-rich stars have [C/Fe]=+0.2, [N/Fe]=+1.3, [O/Fe]=−0.1 and other elements as in the first case.

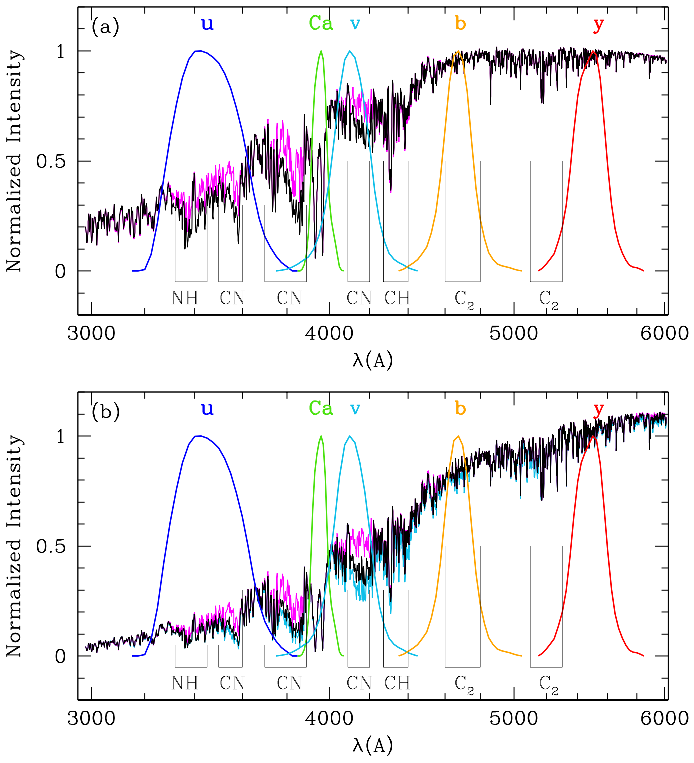

Fig. 12. (a) Synthetic spectra for a N-poor (magenta), a N-rich (black), and a C-rich star at the RGB bump of a GC with [Fe/H]=-1.23 (see Sect. 4 for the various abundances used). Over-imposed are the transmission curves for the *uvbyCa* filters; some features of interest are indicated (see text). (b) The same, but for a star above the RGB bump.

band, and it is then less sensitive to the strength of the CN violet bands. In practice, the sensitivity of δ_4 on CNO abundances is all contained in the $(u - v)$ term. The addition of the $(b - y)$ term is however useful to reduce its sensitivity to temperature and reddening. In particular, since δ_4 is practically insensitive to reddening, it can be safely used also for clusters with strong differential reddening.

5.1. Comparison with Sbordone et al. (2011)

This very recent paper approached the problem of the photometric signatures of multiple populations in GCs from the theoretical point of view. The approach and purposes were different, since the authors wanted to present there full blown isochrones and take the effect of helium in consideration as well,while we concentrated on the RGB. They then computed self-consistent stellar models, taking into account the different chemical composition of first and second generations stars both for the stellar interiors and the stellar atmospheres. They computed models with several composition (standard mixture, NaCNO-enhanced, He-enhanced) and translated the theoretical isochrones into the observational planes for Johnson and Strömgren photometry, showing the effects on the main sequence, SGB, and RGB.

Our paper and theirs, while addressing the same problem, differ in several points: (i) while we have worked on the observational data of several GCs, they did not present a direct comparison with observed cases, deferring this to subsequent papers; (ii) we have not computed new, self-consistent atmospheres and fluxes, but only computed the variation in the absorption spectrum due to a change in composition, using a standard model. Their approach is formally better; however the effect is small, as shown also by their paper, since the molecular bands present in these stars affect only a small fraction of the total flux and the various models differ only in the most external parts, near the stellar surface. In fact, Gustafsson et al. (2008) considered the impact of mild and heavy CN cycling on the structure of the atmospheres and found that it is negligible for the temperatures of interest in our computations (see their Fig. 7); (iii) in our paper the changes in composition due to the first dredge-up and the extra-mixing after the RGB bump are taken into consideration. This has significant impact on the derived results, since C and N are involved in these changes; (iv) perhaps most importantly, they do all calculations only for one value of metallicity, while we explore *the entire range of metallicity of Galactic GCs*. This is an important factor, since we have seen that there is a strong dependence on metallicity of the sensitivity of the various colors and indices to different compositions (see Table 3 and Fig. 13).

Given all these differences, it is legitimate to ask whether we are obtaining similar results. Taking our case at [Fe/H]=−1.63 to compare to their −1.62 and looking at their Fig. 8, we obtain similar, but smaller, differences between N-rich and poor compositions in u (and of course b and y, where N has no influence). There are instead discrepancies in the v filter, where we find differences and they do not. However, there is a large difference in C abundance between the two cases: we use [C/Fe]=−0.2, compared to their −0.6, meaning that their model has [C/H]= −2.23, i.e., is more similar to our [Fe/H]= −2.23 case, where we too do not see any effect in the v filter (the CN bands are really very weak in these models).

The large difference in C abundance and the single, quite low metallicity could also explain the fact that their models predict larger differences in c_y between the different compositions (see their Fig. 15) than our computations (Table 3). In practice, we have stronger CN bands in our spectra and this has an effect on the v filter, that is actually weighted twice in the definition of c_y, and outweighs the effect in the u filter, where the NH band dominates. A more complete comparison between the two works is difficult and outside the goals of the present work. It could be interesting, however, to merge the two approaches, to better define the properties of multiple populations in GCs.

6. Summary

In this paper we explored the capabilities of the Strömgren photometric system to characterize multiple populations that we firmly know (from spectroscopy) to be harbored in *all* GCs. Thanks in particular to the u filter, which encompasses the molecular NH band at 3400 Å, and the v filter, at least for the metal-rich GCs, it is possible to well separate N-poor (Na-poor, O-rich, first generation) stars from N-rich (Na-rich, O-poor, second generation) stars using Strömgren multicolor photometry.

In our systematic exploration of the parameter space, using Grundahl's (and coworkers) photometry made available by Calamida et al. (2007) for 9 GCs, we found that the classical metallicity index m_1 is able, in the present context, to separate in N-strength classes only cool and metal-rich stars.

Both the typical gravity indicator c_1 and its improved version c_y defined by Yong et al. (2008), work well in separating N-rich and N-poor stars at low metallicity, but give ambiguous results in the metal-rich and cool stars regime.

We defined a new indicator, δ_4, that seems to works better than the previous indices over a larger range of metallicity, although even in this case the separation of different populations is not achieved well in the cool and metal-rich regime.

The variations that are sampled by all these indices are well accounted for by changes in the abundances of CNO elements, as demonstrated by a number of comparison with synthetic spectra convolved with the transmission filter. However, further work is necessary, combining for instance our observational approach with the theoretical one chosen by Sbordone et al. (2011).

In the present paper we have limited our analysis to the RGB stars to ensure the best photometric data and to compare directly with the available firm constraints given by the chemical abundances (e.g., the Na-O anticorrelation). The next step will be the extensive analysis of photometric data over wide fields and reaching also extremely blue (faint) HB and main sequence stars with comparable precision. The gain in statistics will permit to better study hot issues such as e.g., the radial distribution of multiple stellar populations in GCs, which is tightly connected with the formation and evolution of these stellar aggregates.

Acknowledgements. We wish to thank the referee Luca Sbordone for his careful report, certainly useful to improve the paper. We used data from the Two Micron All Sky Survey, which is a joint project of the University of Massachusetts and the Infrared Processing and Analysis Center/California Institute of Technology, funded by the National Aeronautics and Space Administration and the National Science Foundation. This research has made use of the SIMBAD and ViZier databases, operated at CDS, Strasbourg, France and of NASA's Astrophysical Data System. Financial support from PRIN-MIUR 2007 "Multiple Stellar Populations in Globular Clusters: Census, Characterization and Origin", and PRIN-INAF 2009 Formation and Early Evolution of Massive Star Clusters", is acknowledged.

References

Anderson, J. 1998, Ph.D. Thesis,
Anthony-Twarog, B. J., & Twarog, B. A. 2000, AJ, 120, 3111
Anthony-Twarog, B. J., Twarog, B. A., Laird, J. B., & Payne, D. 1991, AJ, 101, 1902
Anthony-Twarog, B. J., Twarog, B. A., & Craig, J. 1995, PASP, 107, 32
Anthony-Twarog, B. J., Twarog, B. A., & Mayer, L. 2007, AJ, 133, 1585
Armosky, B. J., Sneden, C., Langer, G. E., & Kraft, R. P. 1994, AJ, 108, 1364
Bedin, L. R., Piotto, G., Anderson, J., Cassisi, S., King, I. R., Momany, Y., & Carraro, G. 2004, ApJ, 605, L125
Bertelli, G., Girardi, L., Marigo, P., & Nasi, E. 2008, A&A, 484, 815
Calamida, A., et al. 2007, ApJ, 670, 400
Carretta, E. 2006, AJ, 131, 1766
Carretta, E., Bragaglia, A., Gratton R.G., Lucatello, S., & Momany, Y. 2007a, A&A, 464, 927
Carretta, E., Bragaglia, A., Gratton, R.G., & Lucatello, S. 2009b, A&A, 505, 139
Carretta, E., Bragaglia, A., Gratton, R., D'Orazi, V., & Lucatello, S. 2009c, A&A, 508, 695
Carretta, E., et al. 2009a, A&A, 505, 117
Carretta, E., Bragaglia, A., Gratton, R.G., et al. 2010, ApJ, 712, L21
Carretta, E., et al. 2010, ApJ, 722, L1
Carretta, E., Lucatello, S., Gratton, R., Bragaglia, A., D'Orazi, V. 2011, A&A, in press (arXiv:1106.3714)
Carretta, E., et al. 2010, ApJ, 714, L7
Carretta, E., Bragaglia, A., D'Orazi, V., Lucatello, S., Gratton, R.G. 2010d, A&A, 519, 71
Carretta, E., Bragaglia, A., Gratton, R.G., Recio-Blanco, A., Lucatello, S., D'Orazi, V., Cassisi, S. 2010c, A&A, 516, 55
Cohen, J. G., & Meléndez, J. 2005, AJ, 129, 303
Decressin, T., Meynet, G., Charbonnel C. Prantzos, N., & Ekstrom, S. 2007, A&A, 464, 1029
D'Ercole, A., Vesperini, E., D'Antona, F., McMillan, S. L. W., & Recchi, S. 2008, MNRAS, 391, 825
Gratton, R. G., Sneden, C., Carretta, E., & Bragaglia, A. 2000, A&A, 354, 169
Gratton, R. G., et al. 2001, A&A, 369, 87
Gratton, R., Sneden, C., & Carretta, E. 2004, ARA&A, 42, 385
Gratton, R. G., Carretta, E., Bragaglia, A., Lucatello, S., & D'Orazi, V. 2010, A&A, 517, A81
Grundahl, F., Briley, M. 2001, NuPhA, 688, 414
Grundahl, F., Catelan, M., Landsman, W.B., Stetson, P.B., Andersen, M.I. 1999, ApJ, 524, 242
Grundahl, F., Stetson, P.B., Andersen, M.I. 2002, 395, 481
Grundahl, F., Vandenberg, D. A., & Andersen, M. I. 1998, ApJ, 500, L179
Gustafsson, B., Edvardsson, B., Eriksson, K., Jørgensen, U. G., Nordlund, Å., & Plez, B. 2008, A&A, 486, 951
Harris, W.E. 1996, AJ, 112, 1487
Johnson, C. I., & Pilachowski, C. A. 2010, ApJ, 722, 1373

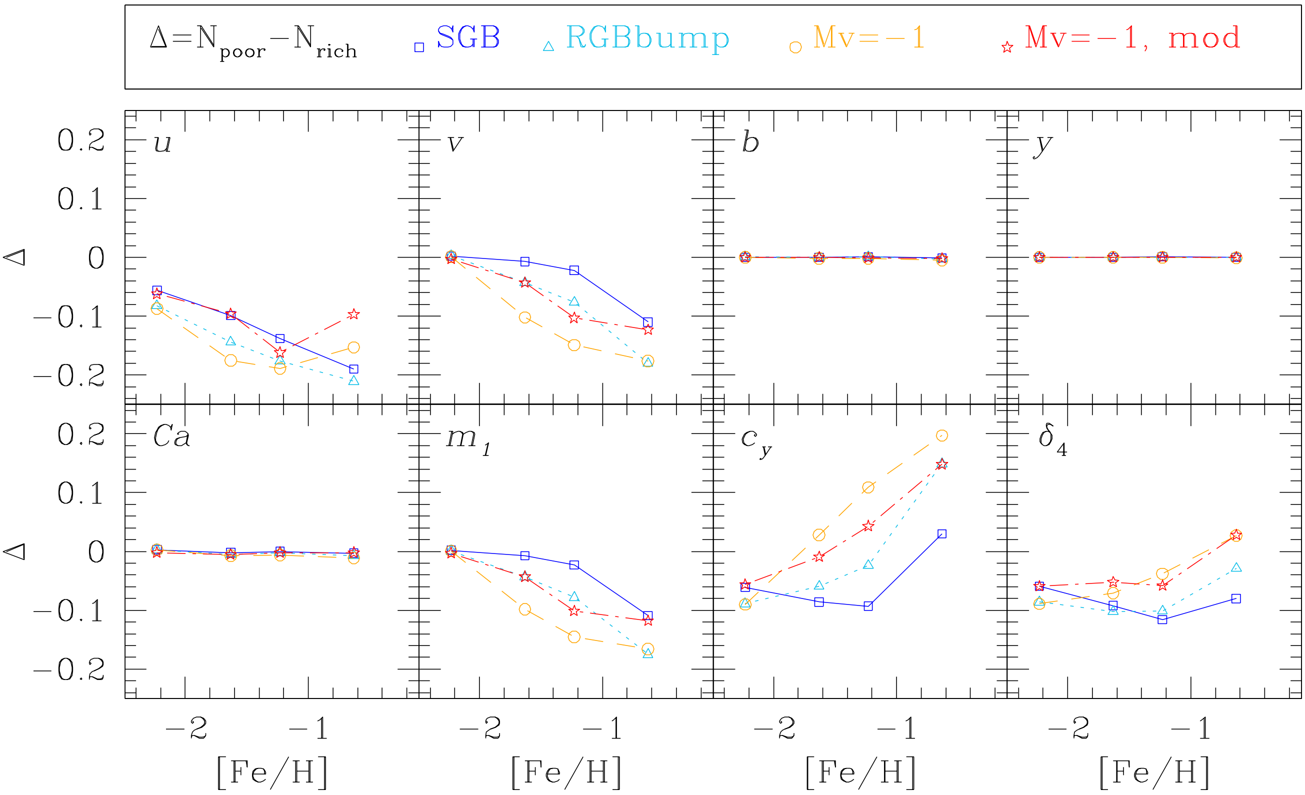

Fig. 13. Run with metallicity of the difference in magnitude and color for "N-rich" and "N-poor" stars (see Table 3). We show the three different evolutionary phases considered (two different compositions for the brighter star, see text). In each panel we indicate the filter/index involved.

Johnson, C. I., Kraft, R. P., Pilachowski, C. A., Sneden, C., Ivans, I. I., & Benman, G. 2005, PASP, 117, 1308

Kravtsov, V., Alcaíno, G., Marconi, G., & Alvarado, F. 2010, A&A, 512, L6

Kurucz, R.L. 1993, CD-ROM 13, Smithsonian Astrophysical Observatory, Cambridge

Lane, R. R., et al. 2010, ApJ, 711, L122

Lardo, C., Bellazzini, M., Pancino, E., Carretta, E., Bragaglia, A., Dalessandro, E. 2011, A&A, 525, 114

Lee, J.-W., Kang, Y.-W., Lee, J., & Lee, Y.-W. 2009, Nature, 462, 480

Lind, K., Primas, F., Charbonnel, C., Grundahl, F., & Asplund, M. 2009, A&A, 503, 545

Lind, K., Charbonnel, C., Decressin, T., Promas, F., Grundahl, F., Asplund, M. 2011, A&A, 527, 148

Marino, A., Villanova, S., Piotto, G., et al. 2008, A&A, 490, 625

Marino, A. F., et al. 2011, ApJ, 731, 64

Moro, D., & Munari, U. 2000, A&AS, 147, 361

Norris, J., & Freeman, K. C. 1979, ApJ, 230, L179

Prantzos, N., & Charbonnel, C. 2006, A&A, 458, 135

Renzini, A. 2008, MNRAS, 391, 354

Sbordone, L., Salaris, M., Weiss, A., & Cassisi, S. 2011, arXiv:1103.5863

Schlegel, D. J., Finkbeiner, D. P., & Davis, M. 1998, ApJ, 500, 525

Skrutskie, M.F. et al. 2006, AJ, 131, 1163

Sneden, C., Pilachowski, C. A., & Kraft, R. P. 2000, AJ, 120, 1351

Sneden, C., Kraft, R. P., Guhathakurta, P., Peterson, R. C., & Fulbright, J. P. 2004, AJ, 127, 2162

Stoughton, C., et al. 2002, AJ, 123, 485

Strömgren, B. 1956, Vistas in Astronomy, 2, 1336

Strömgren, B. 1966, ARA&A, 4, 433

Ventura, P., D'Antona, F., Mazzitelli, I., & Gratton, R. 2001, ApJ, 550, L65

Yong, D., Grundahl, F. 2008, ApJ, 672, L29

Yong, D., Grundahl, F., Johnson, J. A., & Asplund, M. 2008, ApJ, 684, 1159